International Journal of Engineering Trends and Technology
ISSN: 2231–5381 / https://doi.org/10.14445/22315381/IJETT-V72I7P133

Volume 72 Issue 7, 302-311, July 2024

Original Article

Study of Mechanical Properties of Locally Spun Yarn and Woven Fabric Obtained from Sisal Fibers From Njombe-Cameroon

Dydimus NKEMAJA EFEZE[1,2], Anne-Marie NDZIE BIDIMA II[2], Fabien BETENE EBANDA[2], Pierre Marcel Anicet NOAH[2], Abdouramane NSANGOU[2*], Timothée Thierry ODI ENYEGUE[3]

[1]*HTTTC Bambili-University of Bamenda, Cameroon.*
[2]*Laboratory of Mechanical, ENSET, University of Douala, BP, Douala, Cameroon.*
[3]*Laboratory of Energy, Materials, Modeling and Methods, ENSPD, University of Douala, BP, Douala, Cameroon.*

[*]*Corresponding Author : abdouramanensangou791@gmail.com*

Received: 22 March 2024 Revised: 01 June 2024 Accepted: 02 June 2024 Published: 26 July 2024

Abstract *- Since the physical properties of the leaf fibers are not compatible with the mechanisms of industrial cotton spinning and weaving machines, attempts have been made to spin and weave sisal fibers locally. This work aims to characterize the local spun and woven obtained from the sisal fiber. To conduct this study, sisal leaves from the locality of Njombé-Cameroon were used as raw material. Fiber extraction was done by manual scraping technique. The obtained agave sisalana fibers were hand-spun from samples with 04 identical fibers under an "S" direction twist. Different weaves were used to obtain 3 types of fabrics: plain, satin and twill. Similarly, the mechanical properties of the fibers, yarns, and weaves were also studied using a universal tensile testing machine. Statistical analysis of the results revealed an average modulus of elasticity of sisal fibers equal to 1018.72MPa, yarn of 130MPa, whose linear density is 140 Tex and an equivalent tenacity of 694.65 cN/Tex. The average modulus of elasticity of fabrics respectively in the weft and warp direction according to the weaves: plain 31.56 MPa and 29.51 MPa, satin 19.60 MPa and 23.65 MPa, then twill 32.7 MPa and 43.4 MPa. This effectively reflects a variation in mechanical characteristics after each spinning and weaving process.*

Keywords *– Spinning, Weaving, Mechanical Characteristics, Sisal.*

1. Introduction

Biosourced and bi-directional textiles, essentially made up of two networks of yarns (warp and weft) interwoven with each other, have been integrated into several technical fields, particularly the clothing industry, to produce specific materials with high added value that can simultaneously meet consumer requirements. Thanks to the development of their industrial processing techniques, these textiles are used in the form of inputs depending on the characteristics and applications desired in geotextiles (Iryo and Rowe, 2005; Saha et al., 2012; Wu et al., 2020; Wu, 2018), safety, health (Dolez et al., 2018; Panda and Komalavalli, 2019) sport (Chowdhury et al., 2010; Shishoo, 2015), composite materials (Alcaraz et al., 2019; Fangueiro, 2011) (Bahrar, 2018) and many others. To date, to meet specific needs in any of the above-mentioned areas, the development of high-performance fabrics remains a major concern. Recent literature (Fangueiro, 2011; Strumia et al., 2018; Vilfayeau, 2014) shows that depending on the intended field of application, the mechanical characteristics of the textiles to be manufactured are highly dependent on the type of tack chosen (canvas, twill, and satin), the yarn count and the type of twist applied (Alali, 2012). Consequently, the implementation of high-performance bio-sourced two-way textiles would be conditioned by control of the spinning and weaving operations on the one hand and the consequences of the type of tack (canvas, twill, and satin) on the mechanical properties of the fabric obtained on the other. A more recent study (Corbin et al., 2019a, 2020) highlights the influence of the type of weave (satin 6, twill 6, and linen) on the surface density of hemp fabrics in the context of composite reinforcement. Despite the great interest in understanding and controlling the influence of the type of weave (plain, twill, and satin) on the mechanical behaviour of textiles, comparative studies in this field are still very limited to date. The existence of an infinite number of weaves derived from the fundamental weaves (plain, satin, and twill) implies as many interlacings of weft and warp threads as possible and, consequently, a multitude of weaves with varied mechanical characteristics. This study aims to determine the influence of the weaving process on the mechanical characteristics of the resulting weaves. To minimise the errors that can arise from the extraction and industrial weaving processes, the fibers were

extracted by scraping carefully spun locally, and the three types of fabric, which differ in their weaves (plain, satin and twill), were carefully obtained by hand weaving, the constituent yarns of which are composed of 100% sisal fibers from the Njombe region of Cameroon. Tensile tests carried out at fiber, yarn and fabric levels were used to assess the mechanical properties of the textile structures studied. The performance of each fabric in the weft and warp directions was analysed and discussed.

2. Materials and Methods

The material used consists of sisalana agave leaves from the locality of Njombé-Cameroon, fibers, sisal fiber threads, sisal fabrics (canvas, twill and satin), an artisanal woven board, a universal pulling machine.

2.1. Sisal Leaves

Sisal leaves were obtained from a private plantation in the town of Njombe-Cameroon. Figure 1 shows the harvesting area for sisal leaves with an average length of 1.5-1.8 m. The average temperature of this locality is 31°C, with a relative humidity of 73%. The most mature and long leaves were selected.

2.2. Extraction of Sisal Fibers

The fibers were extracted from the leaves after cutting. The extraction operation can be summed up in four stages: threshing in order to eliminate the water and facilitate defibration, and scraping, which makes it possible to extract the fibers. The extracted fibers were rinsed with clean water and finally dried in the open air. Figure 2 shows the different steps of the extraction process. The extracted sisal fibers are in the form of fibrous bundles. After combing and brushing, the individual fibers obtained are shiny and of average length ranging from 1.0 to 1.5 m, with an average diameter of 0.28 to 0.33 mm.

2.3. Tensile Test of Sisal Fibers from Njombé-Cameroon

The tensile tests presented in Figure 3 were carried out on 25 samples of sisal fibers using a universal testing machine LDW-5 according to standard NF T25 501-2. Fiber bundle specimens were fabricated with a gauge length of 10 mm and conditioned in a humidifier for 1 h at 23°C and 50% relative humidity. The test was performed at room temperature (23 ± 1°C and 50 HR) with a constant speed of 2 mm.min -1

2.4. FTIR of Sisal Fibers

FTIR analysis of raw sisal fibers was carried out using a Bruker Alpha-P spectrometer equipped with an ATR module and controlled by Opus/Mentor software. A few milligrams of powder (size ¼ 315 μm) of sisal fibers were scanned over a spectral region from 4000 to 400 cm^{-1} with 32 scans, giving a resolution of 4 cm^{-1}. FTIR spectra were recorded in absorbance mode (FTIR-ATR).

2.5. Thermogravimetric Analysis (TGA)

Thermal properties of sisal fiber samples were determined using a TGA Q50-0836 Instruments thermal analyzer. Samples of 4 mg of sisal fibers ground to a size of 110 μm were heated from room temperature to 650 °C at a heating rate of 10°C.min under a nitrogen atmosphere (flow rate ¼ 10 ml.min).

2.6. Spinning of Yarn

The transformation of sisal fibers into yarn was done by applying a twist. The "S" twist of four fibers was done by hand in order to obtain the most regular yarn.

2.7. Characterization of Sisal Twisted Yarn

The twist level of the yarn was measured according to standard NFG07-079. The modulus of elasticity and the resistance of the thread were determined by means of the tensile test according to the NFG03 standard. 10 specimens were tested using a universal tensile machine LDW-5, with a load cell of 10 kN, gauge length of 200 mm, a speed of movement of the crosshead of 200 mm/min and a preload of 0.5 cN/Tex.

Fig. 1 Sisal sheet supply area

a b c d e

Fig. 2 Steps in the extraction of sisal fibers

Fig. 3 Tensile test of sisal fibers from Njombé-Cameroon

Fig. 4 Traction of sisal fiber weaves

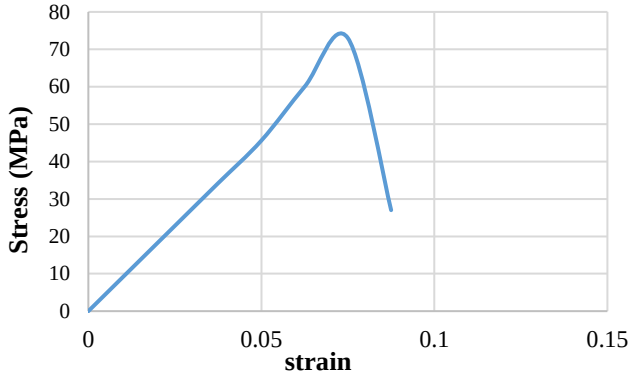

Fig. 5 Graphic representation of the mechanical behavior of sisal fiber

2.8. Method of Weaving

Plain weave, twill and satin fabrics were obtained using a board fitted with hooks serving as a beam on which the warp threads are wound parallel to each other. A network of weft threads was threaded through the eye of a needle to create weft-warp tangles to form the desired fabric. Within the framework of this study, each of the plain, twill and satin weaves was made up of 4 weft threads and 10 warp threads.

2.9. Characterization of Plain, Twill and Satin Woven Fabric

After having obtained the woven fabric, tensile tests (Figure 4) were carried out according to the NFG00 standard in the weft and warp directions respectively. 10 test specimens of 200 mm*25mm*3.2mm and 200 mm*10mm*3.2mm to determine the mechanical properties of each woven fabric.

3. Results and Discussion

3.1. Mechanical characteristics of Sisal Fibers

Figure 5 shows the evolution of the stress as a function of the stain of sisal fibers with an average cross-section of 0.014 mm^2. Results from the mechanical characterization of sisal fibers from Njombe showed it is less ductile with an average modulus of elasticity of 1010 MPa with an average standard deviation of 2. The variation of the characteristics of fibers from Njombé with those obtained from the literature review Table 1 is certainly due to the agricultural techniques, the cultivation area, the degree of maturity of the fibers, the micro fibrillar angle, the level of cellulose present in the fiber, and the degree of crystallinity and the measurement techniques (Ferreira et al., 2015; Radoor et al., 2020; Samouh et al., 2021).

3.2. FTIR Analysis of Sisal Fibers

Figure 6 shows the spectrum obtained from the ATR-FTIR analysis of the sisal fiber. It is observed that raw Sisal fibers show spectra with a similar allure to those of Sida rhombifolia fibers (Ngoup et al. 2024), sisal in a previous study (Seki et al. 2019) and polysaccharides in general (Essome Mbang et al. 2024). The peak located at 3298 cm^{-1} is attributed to hydrogen bonds (OH) in the inter- and intramolecular cellulose network of free hydroxyl groups in hemicellulose (Ngoup et al. 2024). This broad absorption band is characteristic of the presence of liquid water more or less bound to the polymeric network constituted by natural fibers (Célino et al. 2014). The one observed at 2839 cm^{-1} is associated with the asymmetric CH and CH2 stretching vibration present in cellulose and hemicellulose (Kılınç et al. 2018).

Table 1. Summary of physical and mechanical characteristics of sisal fibers

Density (g/ cm^3)	Diameter	Tensile Strength (MPa)	Young's Modulus (GPa)	Elongation at Break (%)	References
1.48-1.50	-	511-635	9.4-22	2-2.5	(Senthilkumar et al., 2022, 2018)
1.33-1.45	-	468-700	9.4-38	2-7	(Neto et al., 2022,2019)
0.113	0.10-0.13(mm)	370	12.5	-	(Okeola et al., 2018)
1.5	-	511-635	4-22	2-2.5	(Veerasimman et al., 2021)
1.450	50-200 (µm)	400-700	9-12	5-14	(Maya et al., 2017)
1.45-1.5	-	350-700	9-22	2-7	(Celino, 2013)
1.450	100-300 (µm)	365	12-25	4-9	(Sreekumar, 2009)
1.279	0.25-0.32 (mm)	436.87	1.01	1.85	This study

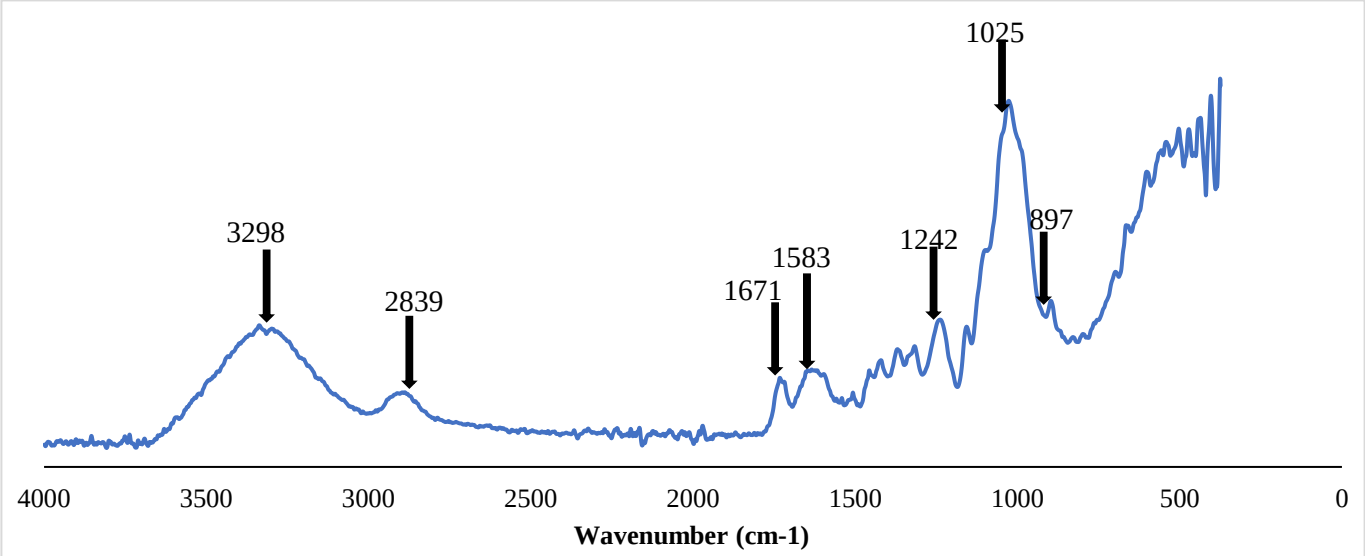

Fig. 6 FTIR of Sisal fibers

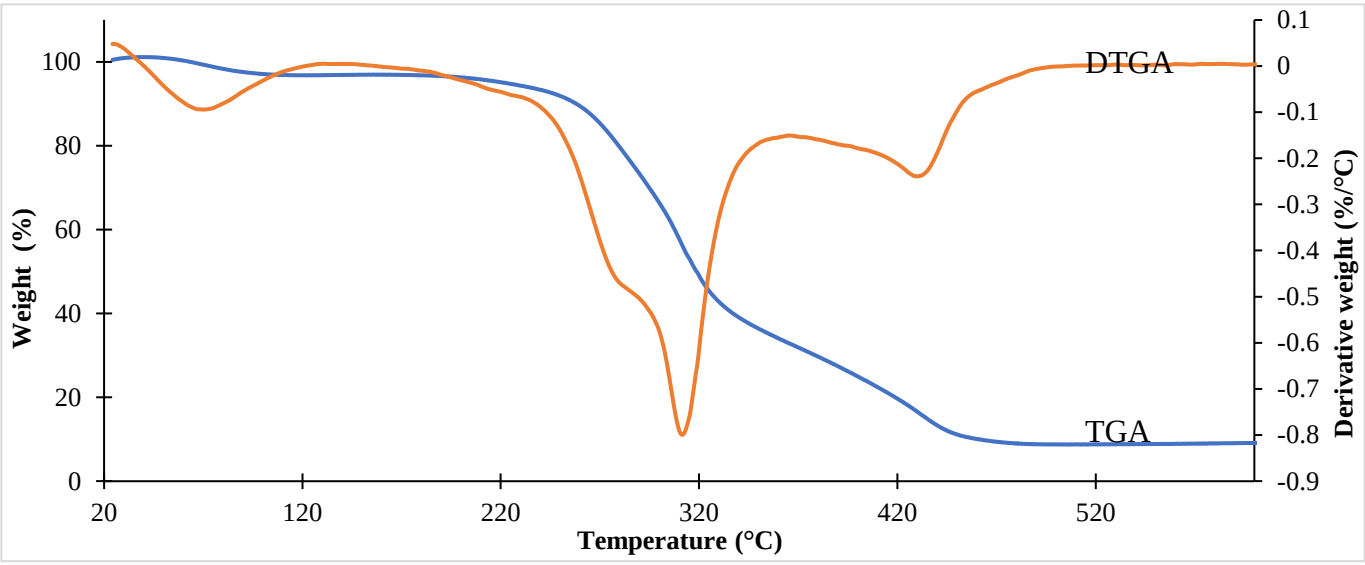

Fig. 7 Thermogravimetric analysis of sisal fibers

The absorption band centered at 1671 cm^{-1} corresponds to the symmetrical ester group (C=O) stretching of the carbonyl groups of hemicelluloses also present in pectins and waxes(Ngoup et al. 2024; Mbere Taoga et al. 2024). The absorbance band at 1583 cm^{-1} is associated with the symmetrical CH2 bending present in cellulose (Moonart and Utara 2019). The peak at 1242 $cm^{-1,}$ characteristic of the vibration of the C-O stretches of the acetyl group, is attributed to hemicellulose and lignin (Obame et al., 2022).

3.3. Thermogravimetric Analysis (TGA)

Figure 7 shows the thermal decomposition (TG) curve coupled with the DSC and DTG curves for sisal fibers. The curve shows the first phase of decomposition, which begins at a temperature of 25°C. At this stage, there is a departure of 3.18% by mass of sisal fiber; this mass corresponds to the evaporation of bound water present in the sisal fiber. Thermal decomposition of sisal fibers occurs in three stages. Interestingly, these fibers exhibit a typical behavior already observed by other authors (Betene et al. 2020) for NA and (Nkapleweh et al. 2022) for Triumpheta. Between 130 and 200°C, the mass loss of the fiber no longer changes. This temperature of 200°C is the thermal stability temperature of sisal fibers, which must be taken into account in the development of composites and textile applications.

The thermal stability of sisal fibers is lower than that of sisal fibers (220 ◦C) in a previous study(Oushabi et al. 2017). This difference could be due to the difference in harvesting location plant maturity. It is also noted that this thermal stability is lower than that of jute (230 ◦C) (Ornaghi Júnior, Zattera, and Amico 2014), kenaf (219 ◦C) (Ornaghi Júnior,

Zattera, and Amico 2014), and Okra (220 ◦C) fibers (Rosa et al. 2008).The second decomposition phase begins after 200°C and ends around 360°C. In this phase, a distinct DTG peak, resulting mainly from the thermal degradation of cellulose (Loganathan et al. 2020), has been observed with a shoulder corresponding to the depolymerization of hemicellulose, pectin and wax reported in the literature (Paul William et al. 2022).

A peak occurs at 308 °C, signaling the end of hemicellulose, pectin and wax decomposition and the start of cellulose decomposition. In fact, when sisal fiber is heated, hemicellulose, pectin and wax are less thermally resistant than cellulose. The final stage of thermal decomposition up to 502 ◦C corresponds to the breakdown of dehydrated products to form volatile products and a discrete graphite layer (Wang et al. 2020). Due to its complex structure, mainly composed of aromatic rings, lignin degradation occurs slowly over the entire temperature range (Lemita et al. 2022; Rosa et al. 2008).

3.4. Mechanical Characteristics of Sisal Yarn

It is noticed from Figure 8 that the yarn obtained is less ductile compared to that of its constituent fibers. However, we noticed that the average value of its modulus of elasticity of 0.13 GPa is significantly different from that of other fibers because of the multiple stages of transformations (combing, twisting) that occurred during the spinning process.; this confirms the assertions of the authors (Almusawi, 2017; Corbin et al., 2019b; Shah et al., 2013).

Furthermore, a comparison of the characteristics of the jute yarn, flax yarn obtained industrially, with that of sisal yarn obtained manually was done Table 2.

3.5. Mechanical Characteristics of the Woven Fabric

Figure 9 shows that the woven fabric in its weft and warp direction has an average Young's modulus of 31.56 MPa with a standard deviation of 7 and 29.51 MPa, respectively, with a standard deviation of 6. Thus, the weft direction is stiffer than the warp direction.

3.6. Mechanical Characteristics of Twill Weave

The twill weave Figure 10 in its weft and warp directions has an average Young's modulus of 43.40 MPa with a standard deviation of 9 and 32.29 MPa, with a standard deviation of 4, respectively. The weft and warp directions of the twill have substantially identical characteristics.

3.7. Mechanical Characteristics of Woven Satin

Figure 11 shows that the woven satin weave in its weft and warp directions has an average Young's modulus of 19.69 MPa with a standard deviation of 9 and 23.65 MPa with a standard deviation of 9, respectively.

3.8. Comparative Analysis of Fibers, Yarn and Woven Fabrics, Twills and Satins

Table 3 shows the decrease in the modulus of elasticity due to the stages involved in the manual method of weaving to obtain the fabric. This result is similar to that of Corbine (2020). The stress exerted on the materials during the various transformations affects their mechanical characteristics. The weft directions of the woven fabrics are more rigid than the warp directions. The twist applied to the fibers during spinning increases the stiffness of the yarn and consequently increases the stiffness of the twill and plain fabric in the weft stiffness direction. The modulus of elasticity equally increased in the warp direction.

Table 2. Comparison of the physical and mechanical characteristics of some plant fiber yarns

Nature yarn	Diameter	Linear Density (tex)	Tenacity (cN/Tex)	Twist (tours/m)	Young's Modulus (GPa)	References
Linen	-	103.3 ± 2,0	-	112 ± 10	1.351 ± 0. 13	(Omrani et al., 2017)
Jute	1,7 mm	-	-	-	0.67	(Ullah et al., 2017)
Sisal-Cameroon	0.32 mm	140	694,65	147.2 ±3,02	0.13 ± 0,02	This study

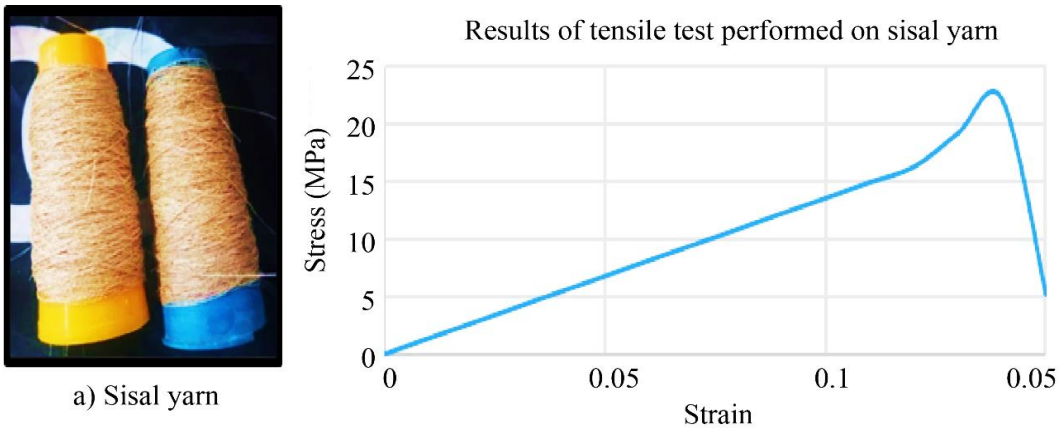

Fig. 8 Graphic representation of the mechanical behavior of sisal yarn with a section of 0.115 mm²

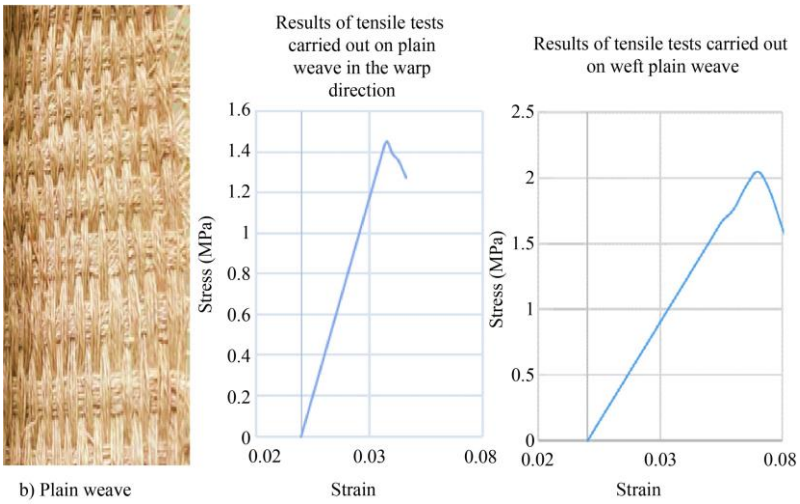

b) Plain weave

Fig. 9 Graphic representation of the mechanical behavior of a fabric structure 32mm thick in tension in its warp and weft direction

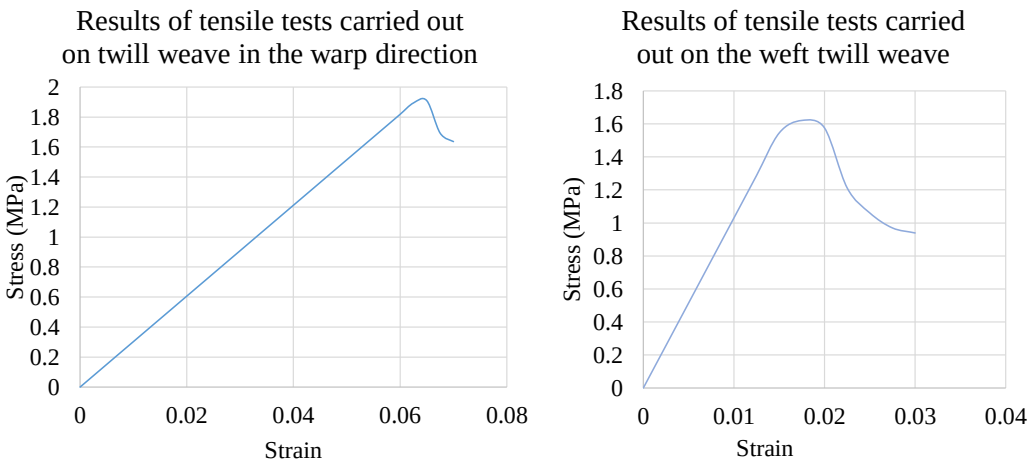

(c) Twill weave 5-2

Fig. 10 Graphic representation of the mechanical behavior of a 32mm thick twill woven fabric

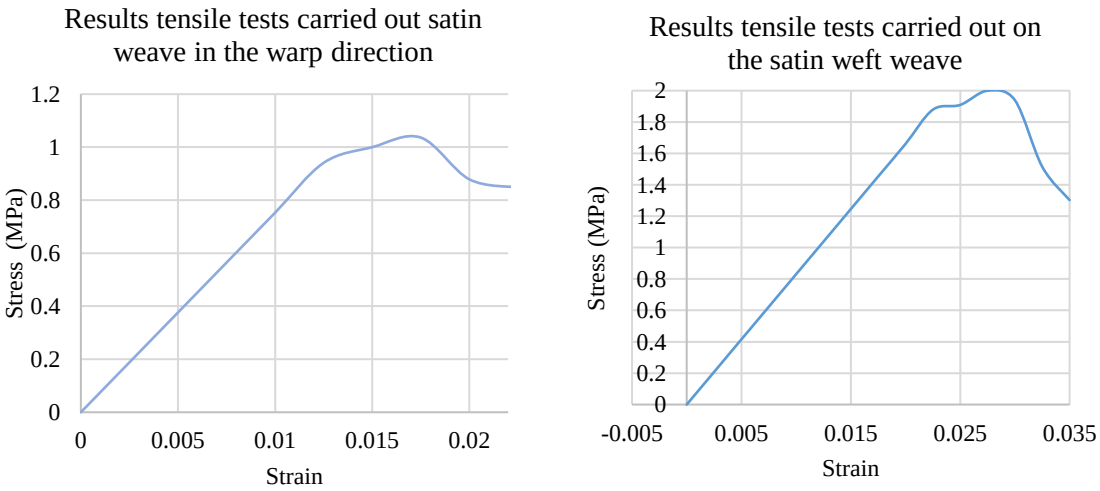

(d) Satin weave

Fig. 11 Graphic representation of the mechanical behavior of a 32mm thick satin fabric

The mechanical characteristics of the fiber, yarn and fabric are shown in Figure 12. Figures 13 and 14 show the elongation at break and stress at break, respectively. The warp direction of woven fabrics has greater elongations than the weft direction, except for the case of satin, whose elongation values are substantially identical. The strains are greater in the warp direction than in the weft direction. Thus, it decreases depending on how the fibers are transformed into yarn and from the yarn to the woven fabric, as shown in Figures 13 and 14. In the case of our woven fabrics, the weft direction has higher breaking stress values than those in the warp direction, as noted for the other characteristics.

Table 3. Comparison of modulus of elasticity and stiffness

Material /Mechanical Properties	Fiber	Yarn	Weft Direction				Warp Direction	
			Canvas Weft	Satin Weft	Twill Weft	Canvas Warp	Satin Warp	Twill Warp
L0 (mm)	20	20	90	90	90	200	200	200
E(MPa)	1018.72	130.72	31.56	19.60	43.40	29.51	23.65	32.29
Rigidity (MPa/mm)	0.71	0.75	0.35	0.21	0.48	0.15	0.11	0.16

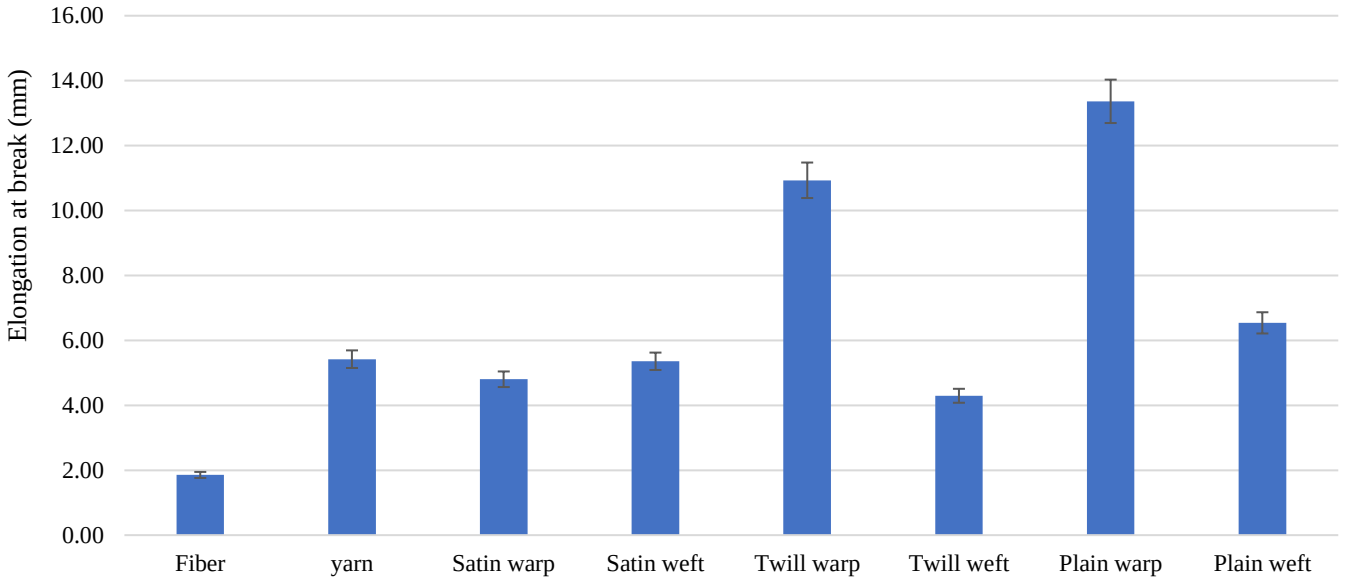

Fig. 12 Elongation at break of fibers, yarn and fabrics

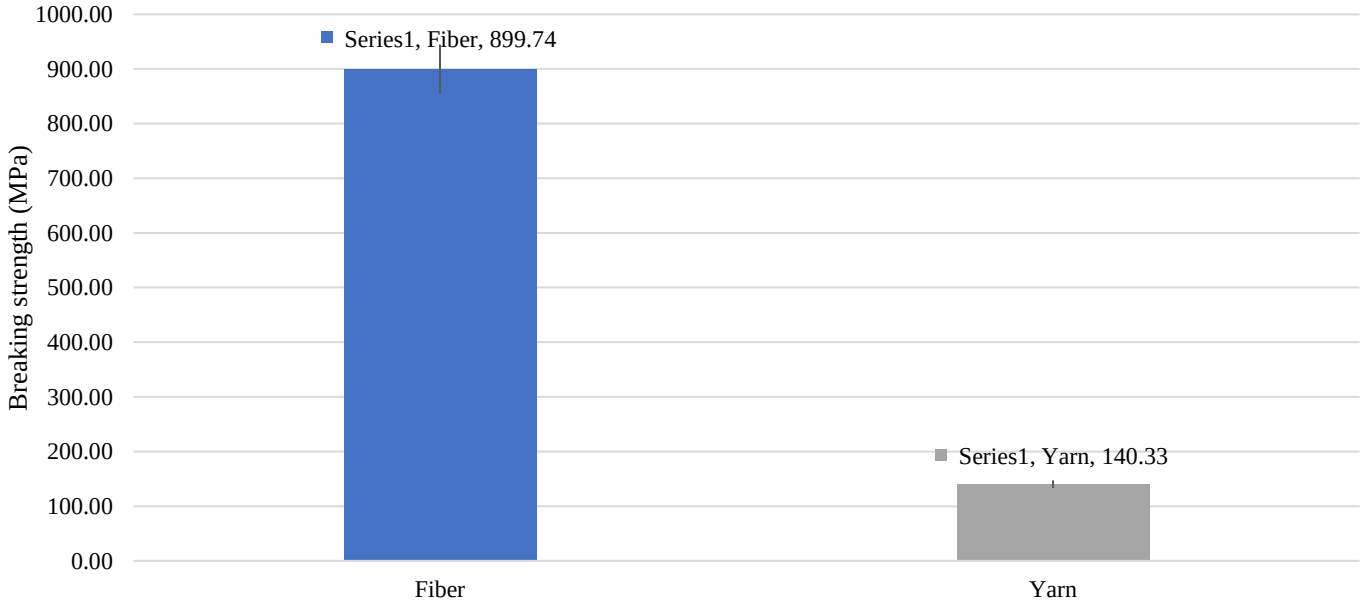

Fig. 13 Stress at break of fiber and yarn

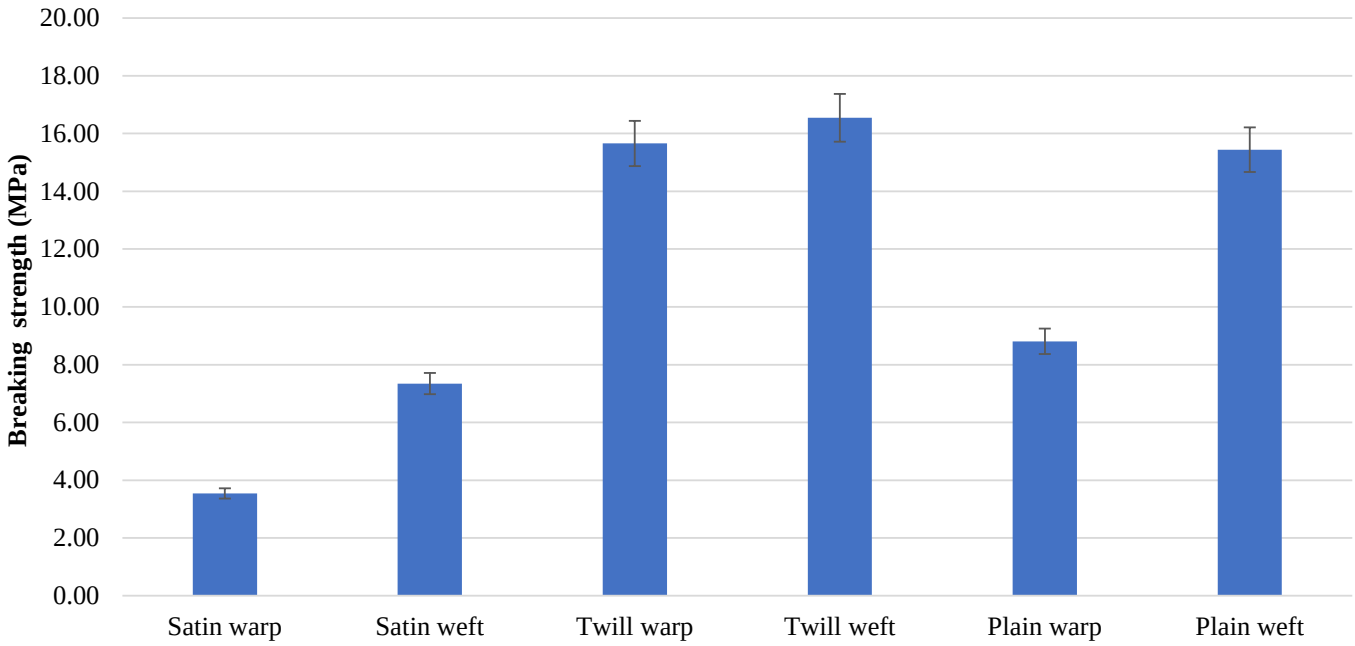

Fig. 14 Stress at break of woven fabrics

4. Conclusion

This work aimed to study the mechanical effects of the transformation of sisal fibers into yarn and yarn into fabric. It appears from this work that: the spinning produces an increase of the rigidity while the weaving causes its decrease resulting in a significant fall of the modulus of elasticity due to the rupture of the threads with the strong constraint exerted at the time of weaving. The weft directions of the said weaves are rigid contrary to the warp directions, except for the case of twill which presents relatively identical characteristics in its two directions. This decrease in mechanical characteristics during the artisanal transformations (spinning and weaving) implies the control of parameters such as: the torsion applied to the fibers during the spinning operation, the orientation of the fibers, their arrangement, the number of entanglements between warp and weft threads in order to hope to produce natural high performance woven fabrics that can be easily integrated in a technical field.

References

[1] Moussa Alali, "*Contribution to the Study of Multilayer Fabrics: CAD and Mechanical Properties*," PhD Thesis, University of Haute Alsace-Mulhouse, pp. 1-226, 2012. [Google Scholar] [Publisher Link]

[2] Jorge Segura Alcaraz et al., "Mechanical Properties of Plaster Reinforced with Yute Fabrics," *Composites Part B: Engineering*, vol. 178, 2019. [CrossRef] [Google Scholar] [Publisher Link]

[3] Aqil Mousa Almusawi, "*Implementation and Optimization of the Properties of a Sandwich Structure Made of Biosourced Materials (Hemp Fibers and Wood) with an Expanded Polystyrene Matrix for Building*," PhD Thesis, Burgundy Franche-Comté University, pp. 1-198, 2017. [Google Scholar] [Publisher Link]

[4] Achille Désiré Omgba Betené et al., "Influence of Sampling Area and Extraction Method on the Thermal, Physical and Mechanical Properties of Cameroonian Ananas Comosus Leaf Fibers," *Heliyon*, vol. 8, no. 8, pp. 1-14, 2022. [CrossRef] [Google Scholar] [Publisher Link]

[5] Amandine Celino, "*Contribution to the Study of the Hygro-Mechanical Behavior of Plant Fibers*," Doctoral thesis, Nantes Central School, 2013. [Google Scholar] [Publisher Link]

[6] Amandine Célino et al., "Qualitative and Quantitative Assessment of Water Sorption in Natural Fibres Using ATR-FTIR Spectroscopy," *Carbohydrate Polymers*, vol. 101, pp. 163-170, 2014. [CrossRef] [Google Scholar] [Publisher Link]

[7] Harun Chowdhury, Firoz Alam, and Aleksandar Subic, "Aerodynamic Performance Evaluation of Sports Textile," *Procedia Engineering*, vol. 2, no. 2, pp. 2517-2522, 2010. [CrossRef] [Google Scholar] [Publisher Link]

[8] Anne-Clémence Corbin et al., "Towards Hemp Fabrics for High-Performance Composites: Influence of Weave Pattern and Features," *Composites Part B: Engineering*, vol. 181, pp. 1-26, 2020. [CrossRef] [Google Scholar] [Publisher Link]

[9] Anne-Clémence Corbin et al., "Improvement of the Weavability of Natural-Fiber Reinforcement for Composite Materials Manufacture," *Review of Composites and Advanced Materials*, vol. 29, no. 4, pp. 201-208, 2019. [CrossRef] [Google Scholar] [Publisher Link]

[10] Patricia Dolez et al., "*Analysis of the Potential of Application of Smart Textiles in Health and Safety at Work*," Robert-Sauvé Research Institute for Occupational Health and Safety, pp. 1-116, 2018. [Google Scholar] [Publisher Link]

[11] Paul Garside, and Paul Wyeth, "Identification of Cellulosic Fibres by FTIR Spectroscopy-Thread and Single Fibre Analysis by Attenuated Total Reflectance," *Studies in conservation*, vol. 48, no. 4, pp. 269-275, 2003. [CrossRef] [Google Scholar] [Publisher Link]

[12] T. Iryo, and R.K. Rowe, "Infiltration into an Embankment Reinforced by Nonwoven Geotextiles," *Canadian Geotechnical Journal*, vol. 42, no. 4, pp. 1145-1159, 2005. [CrossRef] [Google Scholar] [Publisher Link]

[13] Ahmet Çağrı Kılınç et al., "Extraction and Investigation of Lightweight and Porous Natural Fiber from Conium Maculatum as a Potential Reinforcement for Composite Materials in Transportation," *Composites Part B: Engineering*, vol. 140, pp. 1-8, 2018. [CrossRef] [Google Scholar] [Publisher Link]

[14] Nourelhouda Lemita et al., "Characterization and Analysis of Novel Natural Cellulosic Fiber Extracted from Strelitzia Reginae Plant," *Journal of Composite Materials*, vol. 56, no. 1, pp. 99-114, 2022. [CrossRef] [Google Scholar] [Publisher Link]

[15] Tamil Moli Loganathan et al., "Characterization of Alkali Treated New Cellulosic Fibre from Cyrtostachys Renda," *Journal of Materials Research and Technology*, vol. 9, no. 3, pp. 3537-3346, 2020. [CrossRef] [Google Scholar] [Publisher Link]

[16] M.G. Maya et al., "Mechanical Properties of Short Sisal Fibre Reinforced Phenol Formaldehyde Eco-Friendly Composites," *Polymers from Renewable Resources*, vol. 8, no. 1, pp. 27-42, 2017. [CrossRef] [Google Scholar] [Publisher Link]

[17] Ukkadate Moonart, and Songkot Utara, "Effect of Surface Treatments and Filler Loading on the Properties of Hemp Fiber/Natural Rubber Composites," *Cellulose*, vol. 26, no. 12, pp. 7271-7195, 2019. [CrossRef] [Google Scholar] [Publisher Link]

[18] S. Mouhoubi et al., "*Development and Study of the Properties of Treated and Untreated Polyester/ALFA Composites*," Glasses, Ceramics & Composites, vol. 2, no. 1, pp. 34-40, 2012. [Google Scholar] [Publisher Link]

[19] Jorge Neto et al., "A Review of Recent Advances in Hybrid Natural Fiber Reinforced Polymer Composites," *Journal of Renewable Materials*, vol. 10, pp. 561-589, 2022. [CrossRef] [Google Scholar] [Publisher Link]

[20] Abass Abayomi Okeola, Silvester Ochieng Abuodha, and John Mwero, "Experimental Investigation of the Physical and Mechanical Properties of Sisal Fiber-Reinforced Concrete," *Fibers*, vol. 6, no. 3, pp. 1-16, 2018. [CrossRef] [Google Scholar] [Publisher Link]

[21] Heitor Luiz Ornaghi Júnior, Ademir José Zattera, and Sandro Campos Amico, "Thermal Behavior and the Compensation Effect of Vegetal Fibers," *Cellulose*, vol. 21, pp. 189-201, 2014. [CrossRef] [Google Scholar] [Publisher Link]

[22] A. Oushabi et al., "The Effect of Alkali Treatment on Mechanical, Morphological and Thermal Properties of Date Palm Fibers (DPFS): Study of the Interface of DPF–Polyurethane Composite," *South African Journal of Chemical Engineering*, vol. 23, pp. 116-123, 2017. [CrossRef] [Google Scholar] [Publisher Link]

[23] Prasant Kumar Panda, and P. Komalavalli "Health, Social Security and Earnings of Labourers in Informal Sector: Primary Data Evidence from Textile," *Health, Safety and Well-Being of Workers in the Informal Sector in India: Lessons for Emerging Economies*, pp. 13-21, 2019. [CrossRef] [Google Scholar] [Publisher Link]

[24] Paul William Huisken Mejouyo et al., "Experimental Study of Water-Sorption and Desorption of Several Varieties of Oil Palm Mesocarp Fibers," *Results in Materials*, vol. 14, pp. 1-10, 2022. [CrossRef] [Google Scholar] [Publisher Link]

[25] José C. del Río et al., "Composition of Non-Woody Plant Lignins and Cinnamic Acids by Py-GC/MS, Py/TMAH and FT-IR," *Journal of Analytical and Applied Pyrolysis*, vol. 79, pp. 1-2, pp. 39-46, 2007. [CrossRef] [Google Scholar] [Publisher Link]

[26] D.S. Rosa et al., "Evaluation of Enzymatic Degradation Based on the Quantification of Glucose in Thermoplastic Starch and its Characterization by Mechanical and Morphological Properties and NMR Measurements," *Polymer Testing*, vol. 27, no. 7, pp. 827-834, 2008. [CrossRef] [Google Scholar] [Publisher Link]

[27] Prosenjit Saha et al., "Durability of Transesterified Jute Geotextiles," *Geotextiles and Geomembranes*, vol. 35, pp. 69-75, 2012. [CrossRef] [Google Scholar] [Publisher Link]

[28] Zineb Samouh et al., "Identification of the Physical and Mechanical Properties of Moroccan Sisal Yarns Used as Reinforcements for Composite Materials," *Fibers*, vol. 9, no. 2, pp. 1-16, 2021. [CrossRef] [Google Scholar] [Publisher Link]

[29] Yasemin Seki et al., "Characterization of Flax, Jute, and Sisal Fibers After Sodium Perborate Modification," *AATCC Journal of Research*, vol. 6, no. 6, pp. 25-31, 2019. [CrossRef] [Google Scholar] [Publisher Link]

[30] K. Senthilkumar et al., "Mechanical Properties Evaluation of Sisal Fibre Reinforced Polymer Composites: A Review," *Construction and Building Materials*, vol. 174, pp. 713-729, 2018. [CrossRef] [Google Scholar] [Publisher Link]

[31] K. Senthilkumar et al., "Dual Cantilever Creep and Recovery Behavior of Sisal/Hemp Fibre Reinforced Hybrid Biocomposites: Effects of Layering Sequence, Accelerated Weathering and Temperature," *Journal of Industrial Textiles*, vol. 51, pp. 2372S-2390S, 2022. [CrossRef] [Google Scholar] [Publisher Link]

[32] Darshil U. Shah, Peter J. Schubel, and Mike J. Clifford, "Modelling the Effect of Yarn Twist on the Tensile Strength of Unidirectional Plant Fibre Yarn Composites," *Journal of Composite Materials*, vol. 47, pp. 425-436, 2013. [CrossRef] [Google Scholar] [Publisher Link]

[33] P.A. Sreekumar et al., "Effect of Fiber Surface Modification on the Mechanical and Water Absorption Characteristics of Sisal/Polyester Composites Fabricated by Resin Transfer Molding," *Composites Part A: Applied Science and Manufacturing*, vol. 40, pp. 1777-1784, 2009. [CrossRef] [Google Scholar] [Publisher Link]

[34] Miriam C. Strumia et al., "Polymeric Biomaterials: The Giants Born from a Multidisciplinary Challenge," *Digital Log*, vol. 1, no. 9, pp. 1-8, 2018. [Google Scholar] [Publisher Link]

[35] Arumugaprabu Veerasimman et al., "Thermal Properties of Natural Fiber Sisal Based Hybrid Composites – A Brief Review," *Journal of Natural Fibers*, vol. 19, no. 12, pp. 4696-4706, 2021. [CrossRef] [Google Scholar] [Publisher Link]

[36] Jérôme Vilfayeau, "*Digital Modeling of the Weaving Process of Fibrous Reinforcements for Composite Materials*," PhD Thesis, pp. 1-152, 2014. [Google Scholar] [Publisher Link]

[37] Weiming Wang et al., "Changes in Physicomechanical Properties and Structures of Jute Fibers After Tetraacetylethylenediamine Activated Hydrogen Peroxide Treatment," *Journal of Materials Research and Technology*, vol. 9, no. 6, pp. 15412-15420, 2020. [CrossRef] [Google Scholar] [Publisher Link]

[38] Hao Wu et al., "Review of Application and Innovation of Geotextiles in Geotechnical Engineering," *Materials*, vol. 13, no. 7, pp. 1-21, 2020. [CrossRef] [Google Scholar] [Publisher Link]

[39] Jiaping Wu, "*Study of the Fatigue Behavior of Woven Composites and Determination of Damage Initiation Thresholds*," PhD Thesis, University of Sherbrooke, pp. 1-168, 2018. [Google Scholar] [Publisher Link]